Journal of Sustainable Metallurgy (2023) 9:678–687
https://doi.org/10.1007/s40831-023-00672-7

RESEARCH ARTICLE

Electrochemical Kinetics Study of Ultrasound-Assisted Chalcopyrite Oxidation

Lin Li[1] · Aaron King[1] · Krystal Davis[1] · Ben Yu[1]

Received: 12 October 2022 / Accepted: 1 March 2023 / Published online: 3 April 2023
© Crown 2023

Abstract

Ultrasound-assisted chalcopyrite leaching has been reported previously, showing a noticeable improvement in leaching kinetics. However, the effect of ultrasound on the chalcopyrite oxidation kinetics from an electrochemical perspective has not been addressed. This study examines the ultrasonic enhancement of chalcopyrite oxidation kinetics in sulfuric acid solution from both conventional leaching and electrochemistry aspects. Electrochemical techniques, including linear sweep voltammetry (LSV) and chronoamperometry (CA), were used to illustrate the kinetics of chalcopyrite ultrasound-assisted leaching. Tafel analysis by LSV showed that 20% amplitude ultrasound power had increased the chalcopyrite electrochemical dissolution rate by about 20% in both Fe^{3+}-free and 10 mM Fe^{3+}-containing 0.5 M sulfuric acid solution. The CA tests indicated a drastic increase in the Fe^{3+} reduction reaction when ultrasound was applied (20% amplitude). At 0.5 V, the Fe^{3+} to Fe^{2+} reduction current density at 30 min drastically increased from – 65.54 without ultrasound to – 1165.84 μA cm^{-2} with ultrasound.

Graphical Abstract

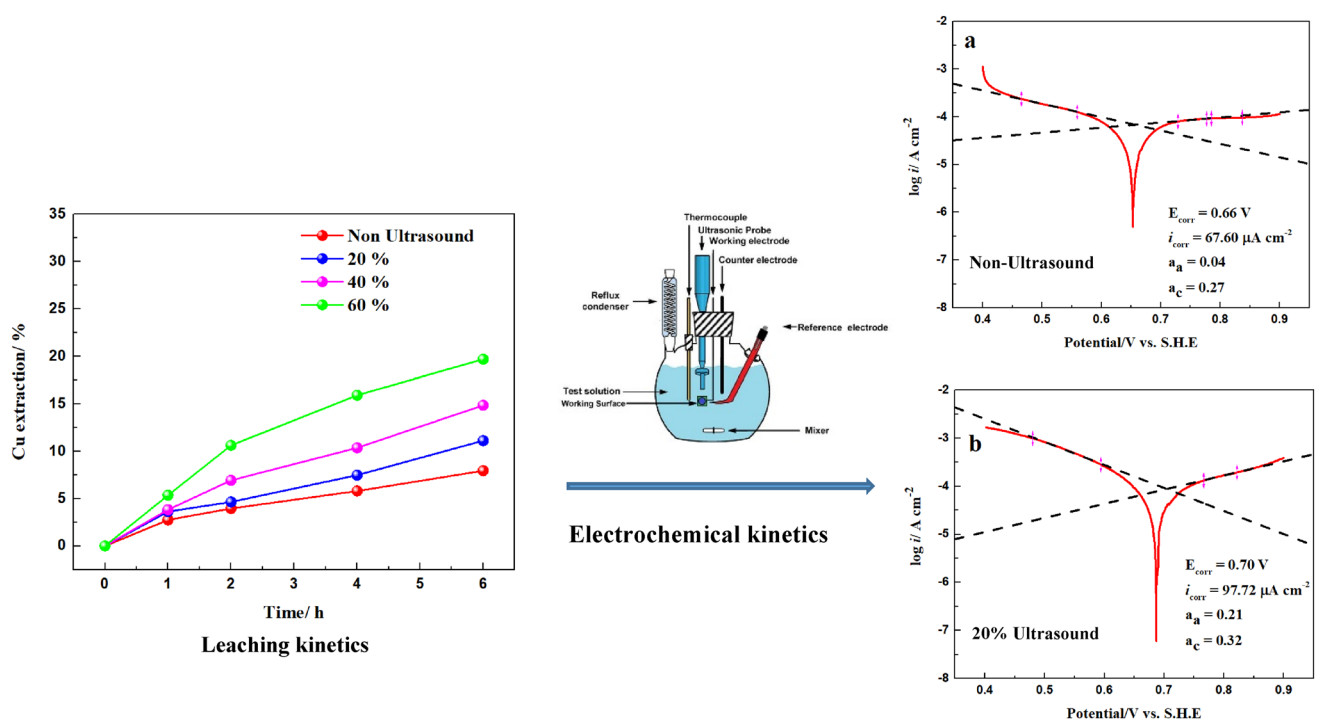

The contributing editor for this article was Hojong Kim.

Extended author information available on the last page of the article

Keywords Chalcopyrite · Ultrasound · Linear sweep voltammetry · Tafel kinetics · Chronoamperometry · Leaching

Introduction

Chalcopyrite accounts for 70% of global copper resources, and more the 90% of the chalcopyrite is treated by the pyrometallurgical process [1]. However, the depletion of high-grade copper deposits brings challenges to traditional pyrometallurgical operations, especially with the high amounts of deleterious impurities, such as arsenic. In addition, the increasing demand for environmentally friendly processes is driving the industry to an efficient hydrometallurgical processing strategy [2].

Chalcopyrite leaching is typically done under acidic conditions (pH < 2), and different acid media such as chlorine and sulfate have been intensively studied [3]. Chalcopyrite leaching in chlorine media has the advantage of conducting under normal pressure; however, the system can be highly corrosive. Recent research explored the additive of NaCl or brine solution to participate in the leaching of chalcopyrite, which is much less corrosive than in the HCl media. Sulfate-based acid leaching is attractive to researchers due to less corrosive, more economical, and ease of electrowinning high-grade copper compared to chloride solution [4–9]. However, the atmospheric leaching of chalcopyrite in sulfuric acid media suffers from slow dissolution kinetics [2, 10–13]. The reason has been widely debated, mainly attributed to its crystallographic structure and passive layer formation on the chalcopyrite surface during leaching [14–16]. However, the composition of this passive layer and the intrinsic oxidation mechanism has not reached any firm conclusions. Different approaches, including pressure leaching [17], strong oxidants (H_2O_2, O_3) [18, 19], and catalysts (Ag^+, pyrite, Cl^-) [16, 20, 21], have been attempted to enhance chalcopyrite leaching in sulfuric acid solution. Turan et al. studied the chalcopyrite under pressure-leaching conditions. At 60 °C, 3 M H_2O_2 as oxidant, 88.5% Cu could be extracted after 3 h. Wang et al. explored using O_3 on chalcopyrite leaching. When at room temperature, 10.1 mg/L O_3, and pulp density of 5 g/L, 100% recovery of Cu was achieved after 48 h without addition of Fe^{3+}. However, the high capital cost of pressure reactor, expensive catalysts or chemical reagents, redundant procedures, and easy-to-decompose of O_3 and H_2O_2 limited their further application.

Ultrasound-assisted leaching (UAL) has demonstrated to enhance chemical leaching with compelling advantages, such as low cost, reduce leach time, being environmentally friendly, and low energy consumption [22–24]. Factors affecting UAL of chalcopyrite, including sonication power, temperature, particle size, and type of oxidant have been explored for UAL of chalcopyrite [25–27]. Yoon et al. investigated the UAL of chalcopyrite in $FeCl_3$-HCl solution with 5 W sonication power. They found that Cu extracted increased from 77 to 87% in alkaline media with ultrasound at optimal conditions [26]. Turan et al. found that application of ultrasound promoted the efficiency of chalcopyrite leaching with chelating agents, e.g., EDTA, titriplex III, etc. [28]. At optimal conditions, the copper and iron extraction could be 93% and 65%, respectively, at the reaction temperature of 45 °C. Wang et al. studied the effect of ultrasound on chalcopyrite leaching in acidic ferric sulfate media [27]. The results showed that the Cu extraction increased from 50.4 to 57.5% with 20% amplitude power. However, previous studies only demonstrated the effectiveness of ultrasound-assisted chalcopyrite leaching from the perspective of leaching kinetics, neglecting that chalcopyrite oxidation is an essential electrochemical process with complex electron transfer processes [29]. The overall chalcopyrite leaching can be represented as a combination of anodic and cathodic half-cell reactions. The anodic reaction is the chalcopyrite oxidation:

$$CuFeS_2 \rightarrow Cu^{2+} + Fe^{2+} + 2S^0 + 4e^-. \quad (1)$$

While the cathodic reaction is the oxidant reduction reaction, for example, Fe^{3+} reduction

$$Fe^{3+} + e^- \rightarrow Fe^{2+}. \quad (2)$$

Based on the mixed potential theory [30], the chalcopyrite dissolution process reaches a mixed potential when the sum of all anodic reaction rates is equal to the sum of all cathodic reaction rats. At such steady state, the total rate of electrode (chalcopyrite) dissolution rate follows chalcopyrite anodic oxidation rate. Therefore, it is possible to conclude the kinetics of the chalcopyrite leaching process with individual electrode reactions. Factually, many studies have been conducted on the electrochemical mechanism and kinetics study of chalcopyrite extraction [7, 31–33]. Electrochemical studies have shown that the poor chalcopyrite leaching kinetics is generally related to the passivated anodic reaction [7, 14].

In order to further explore the application of ultrasound on chalcopyrite oxidation, this study, for the first time, investigates the kinetics of ultrasound-assisted chalcopyrite oxidation from the perspective of electrochemistry by using different electrochemical techniques. Linear sweep voltammetry (LSV) with the Tafel analysis was used to determine the dissolution rate of chalcopyrite with and without ultrasound

in sulfuric media. Chronoamperometry (CA) was applied to compare the chalcopyrite anodic or oxidant (Fe^{3+}) cathodic behaviors at different applied potentials with and without ultrasound. Conventional UAL of chalcopyrite tests with and without ultrasound were also conducted for comparison.

Experimental

Mineral Preparation

The chalcopyrite leaching and electrochemical tests were conducted on chalcopyrite concentrates originating from Mexico. The bulk chalcopyrite was crushed, pulverized, and sieved to obtain a particle size in the range of + 53/ − 75 µm.

The crystallographic structure of the mineral was characterized by X-ray diffraction (XRD) using a Bruker D8 Advance powder diffractometer and Cu kα radiation. A secondary scan with a cobalt radiation tube was used to counteract background noise caused by the high iron content. The particle size of the concentrates was further determined by the Partica LA-950 Laser Diffraction Particle Size Distribution Analyzer. The Cu content in the mineral was measured by atomic absorption spectroscopy (AAS) using a SpectrAA 55B instrument after acid digestion with aqua regia, filtration, and dilution.

Chalcopyrite Leaching Tests

The chalcopyrite leach tests were conducted in a 500 mL reactor with a controlled heating mantle. The temperature for the leach tests with and without ultrasound was set at 60 °C. An ultrasonic processor (VC 750 model, Sonics & Materials Inc. USA) constantly delivered the ultrasound with a standard microtip of 13 mm immersed in the solution. The effects of the sonication power and S/L (solid/liquid) ratio on UAL of chalcopyrite in Fe^{3+}-containing sulfuric acid solution were explored. The sonication power input was adjusting the amplitude of the sonicator probe, and at an amplitude of 20% to 60% with a step of 20%. The sonication frequency was set as a constant frequency of 20 kHz for all the leach and electrochemical tests. The reaction time was set as 6 h, and the mixing rate was 600 rpm for leaching tests. During the leaching tests, sampling was performed at 1, 2, 4, and 6 h. Slurry (less than 3 mL) was withdrawn and subjected to centrifugation, filtration, dilution, and final Cu concentration measurement using AAS. The following equation determined the Cu leached%:

$$\text{Cu leached\%} = \frac{\text{Cu weight dissolved}}{\text{Total Cu weight}} \times 100\%. \quad (3)$$

Electrochemical Tests

The ultrasound in chalcopyrite electrochemical behavior study was conducted by a Princeton applied research 273A potentiostat in Fe^{3+}- free and Fe^{3+}-containing sulfuric acid solution. A conventional 3-electrode system was used. The working electrode was made from the chalcopyrite concentrate. The fabrication method was explained elsewhere [34], and 1 cm^3 of the surface was exposed to the electrolyte. The reference electrode was a saturated calomel electrode (SCE) with saturated KCl as the internal solution, 0.241 V versus SHE (standard hydrogen electrode) at 20 °C. All the potential in this paper refers to versus SHE. For an elevated temperature, the correction of the measured potential was adjusted by Eq. 2 [35], where E_{SCE} is the standard potential of the reference electrode as a function of temperature, and T is degrees Celsius:

$$\begin{aligned} E_{SCE}(\text{V}) = 0.2412 &- 0.661 \times 10^{-3}(T-25) \\ &- 1.75 \times 10^{-6}(T-25)^2 \\ &- 9.0 \times 10^{-10}(T-25)^3. \end{aligned} \quad (4)$$

At 60 °C, E_{SCE} was calculated to be 0.216 V. The counter electrode was a Pt mesh electrode. All the electrochemical tests were conducted at 60 °C. Prior to the electrochemical tests, the chalcopyrite electrode was stabilized with applied ultrasound in the electrolyte, and the open-circuit potential (OCP) was monitored. The electrochemical measurements started only when the OCP was stabilized within ± 2 mV in 5 min.

Linear sweep voltammetry (LSV) with Tafel analysis was carried out to obtain the chalcopyrite electrochemical oxidation kinetics with and without ultrasound (20% amplitude). The LSV test scan started from 0.4 V and ended at 0.9 V with a scan rate of 10 mV s^{-1}. Chronamperometry tests were carried out using the same set-up at applied potentials of 0.5, 0.6, 0.7, and 0.8 V for 30 min. For the ultrasonic-electrochemical tests, the ultrasound (20% amplitude) was performed during both the OCP measurement and CA tests.

Results and Discussion

Chalcopyrite Ore Characterization

The XRD pattern of the mineral is shown in Fig. 1a. Quantitative XRD analysis by Bruker EVA software showed that the sample contained 65.6% chalcopyrite (PDF#37-0471), 19.1% pyrite (PDF#42-1340), and 18.9% quartz (PDF#49-1045). Cu concentration measurement by AAS showed that it contained 24.32% of Cu. Particle analysis (Fig. 1b)

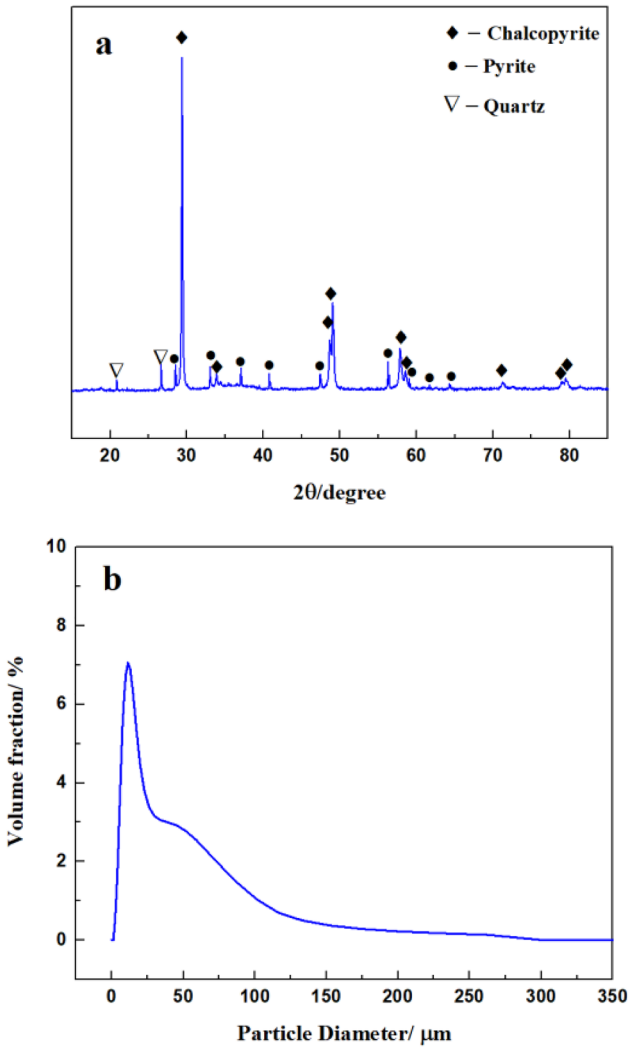

Fig. 1 **a** X-ray diffraction pattern and **b** particle size distribution of the chalcopyrite concentrates

demonstrated that the average diameter of the treated mineral was about 23.52 μm, and the P80 was approximately 82.86 μm.

Ultrasound-Assisted Leaching Kinetics

Effect of Sonication Power

The amplitude of the ultrasound regulated the cavitation intensity within liquid. The effect of sonication power tests compared the ultrasound at 0, 20, 40, and 60% amplitudes for chalcopyrite leaching at the S/L ratio of 10%, room temperature. The Cu% extracted within 6 h are presented in Fig. 2.

As can be seen, the Cu extracted% gradually increased with the increasing sonication power. When no ultrasound was applied, only 7.95% of Cu was leached after 6 h.

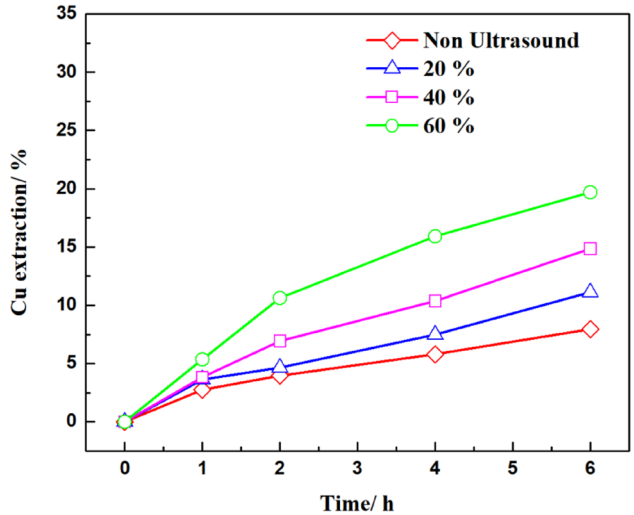

Fig. 2 Effect of sonication power (amplitude%) on chalcopyrite leaching in 10 mM Fe^{3+}-containing 0.5 M sulfuric acid solution, S/L = 10%

Increased sonication power to 60% amplitude, amount of Cu extracted was raised to 19.70%, which is about 2.5 times comparing to the non-UAL test. The results confirmed the positive effect of ultrasound brought on chalcopyrite oxidation, which is consistent with previous studies [26, 27]. The increase could be explained as ultrasound accelerated the Fe^{3+} reduction process on the chalcopyrite surface, hence, the whole chalcopyrite oxidation process. As mentioned above, the essential electrochemical process contained two half-reactions: chalcopyrite oxidation and Fe^{3+} reduction. The verification of assumption will be verified in the electrochemical part of this study. Another reason could be the high-intensity ultrasound partially removed the passive film built on the chalcopyrite surface, which needs to be further explored with multiple spectroscopy methods.

Effect of the S/L Ratio

The S/L ratio is essential for the ultrasound-assisted solid–liquid extraction process. A high S/L ratio slurry could cause enhanced probe corrosion [36]. Figure 3 shows the UAL of chalcopyrite at S/L ratios of 0.5, 2, 5, and 10%, with 20% amplitude sonication power within 6 h. Figure 4 compares the final Cu% leached after 6 h. As can be seen, ultrasound increased the chalcopyrite leaching at all S/L ratios compared to non-ultrasound tests. Decreasing the S/L ratio from 10 to 0.5%, the Cu leached% rose from 4.21 to 17.00 without ultrasound and rose from 8.13 to 24.61 with 20% amplitude ultrasound. The reasons can be explained as reduced slurry viscosity and eliminated diffusion barriers of the low S/L ratio [27].

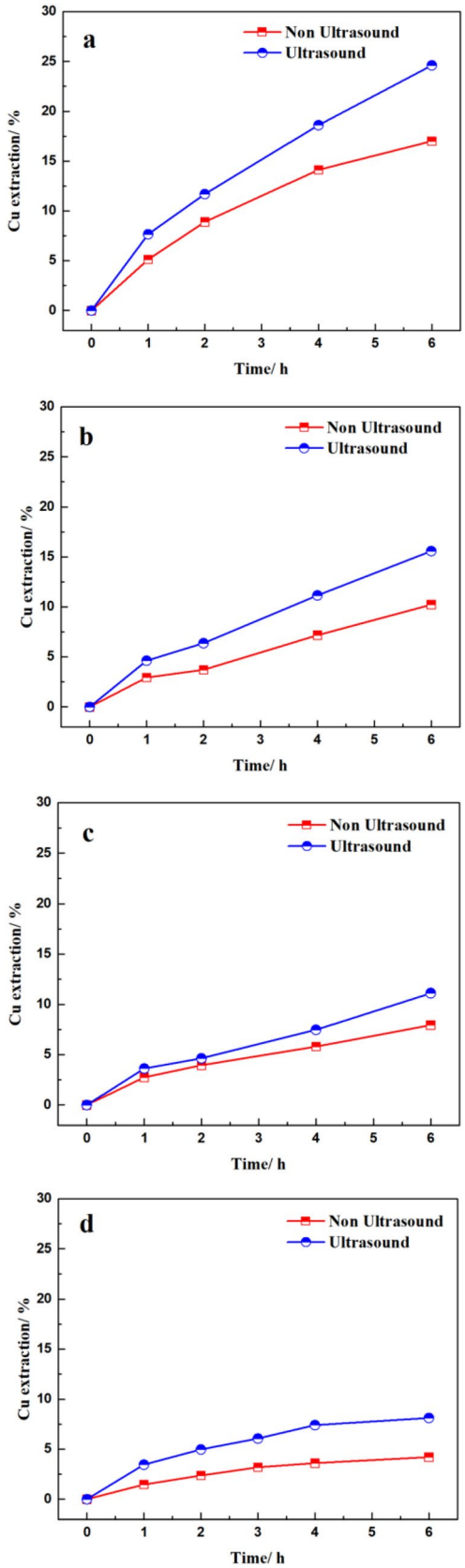

Fig. 3 Effect of S/L ratio on UAL of chalcopyrite: Cu extraction in 10 mM Fe^{3+} containing 0.5 M sulfuric acid solution with 20% amplitude sonication power: **a** 0.5%, **b** 2%, **c** 5%, **d** 10%

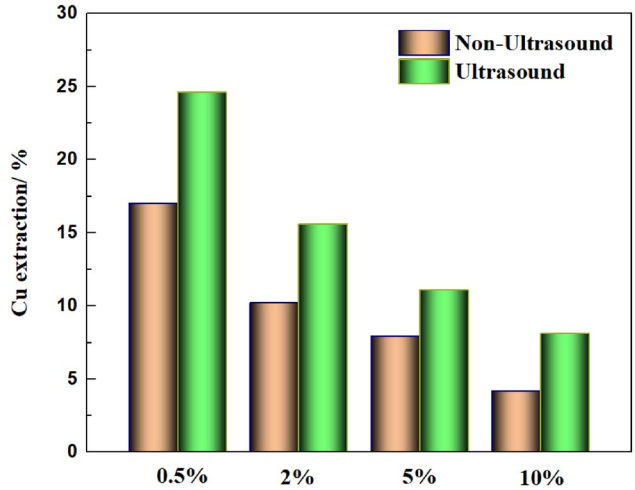

Fig. 4 Comparation of Cu% leached with and without ultrasound (20% amplitude) for chalcopyrite leaching in 10 mM Fe^{3+} containing 0.5 M sulfuric acid solution after 6 h

Electrochemical Analysis

Chalcopyrite Dissolution Tafel Analysis

The electrochemical kinetics of chalcopyrite dissolution with and without ultrasound was measured by LSV and interpreted by Tafel analysis. The Tafel equation can be written as follows [37]:

$$i = i_0 e^{-\alpha f \eta}, \tag{5}$$

where i_0 (i_{corr}) is the exchange current density, α is the charge transfer coefficient, $f = F/RT$, F is the Faraday's constant, R is the gas constant, T is the temperature in K, η is the overpotential ($E - E_{corr}$). E_{corr} is the equilibrium potential. i_{corr} and E_{corr} can be determined by the intersection of anodic and cathodic Tafel lines. For the anodic and cathodic half-reactions, their relative Tafel equation can be written as follows:

$$\log i_A = \log i_0 + \frac{\alpha_a nF\eta}{2.3RT}, \tag{6}$$

$$\log -i_C = \log i_0 - \frac{\alpha_c nF\eta}{2.3RT}, \tag{7}$$

where i_A is the anodic current density, i_C is the cathodic current density, α_a and α_c are the anodic and cathodic transfer coefficient, respectively. Figure 5 shows the Tafel curves of chalcopyrite oxidation in 0.5 M sulfuric acid solution with and without ultrasound (20% amplitude).

The Tafel analysis in Fig. 5 indicated that the 20% amplitude ultrasound had increased the chalcopyrite's electrochemical dissolution. The i_{corr} of chalcopyrite in Fe^{3+}-free acid solution boosted from 39.55 to 57.54 μA

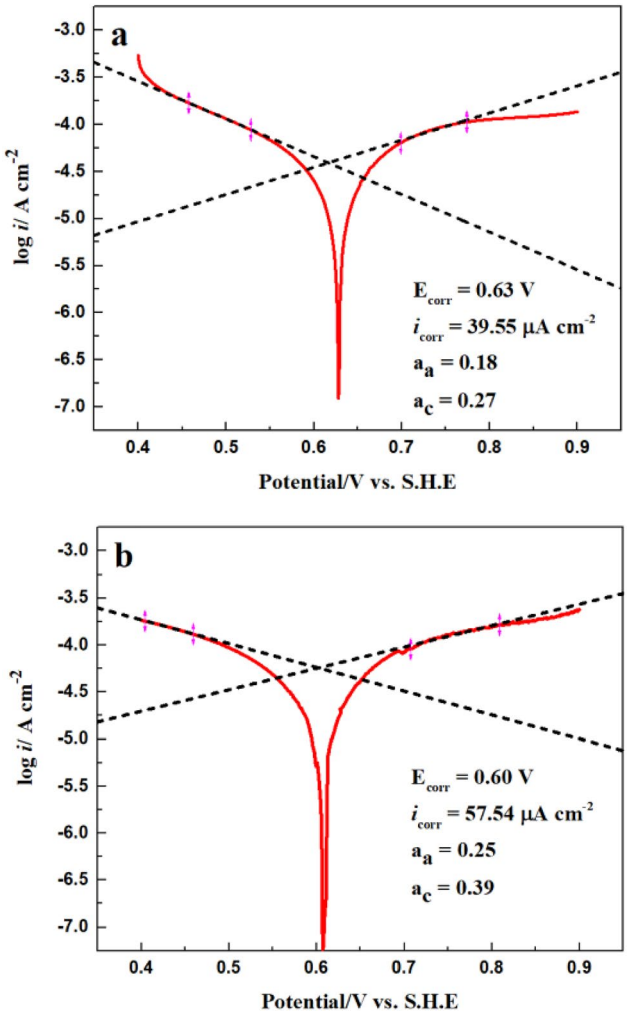

Fig. 5 Polarization curves and Tafel analysis of chalcopyrite in Fe^{3+}-free 0.5 M sulfuric acid solution **a** without ultrasound and **b** with ultrasound (20% amplitude)

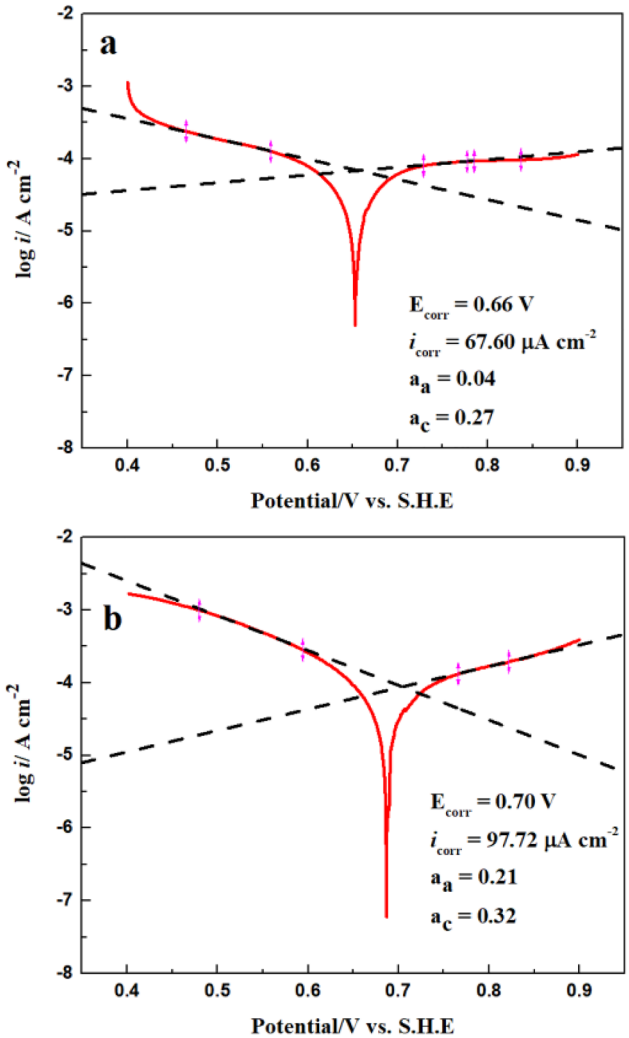

Fig. 6 Polarization curves and Tafel analysis of chalcopyrite in 10 mM Fe^{3+} containing 0.5 M sulfuric acid solution **a** without ultrasound and **b** with ultrasound (20% amplitude)

cm^{-2} (45% increase) after the ultrasound was added. As for the equilibration potential, the E^0 shifted from 0.63 V without ultrasound to 0.60 V with ultrasound. The charge transfer coefficients in both graphs showed $\alpha_a < \alpha_c$, which has been generally considered as an indication of n-type semiconductor properties. In this case, more overpotential is needed for chalcopyrite oxidation since most of it has to overcome the electrostatic force and prompt the diffusion of the electron onto the surface of chalcopyrite. On the other hand, the cathodic process, i.e., O_2 or Fe^{3+} reduction reaction, has few obstacles. This study shows the same trend compared to previous reports [38, 39]. Also, it was also found that the ultrasound had increased both α_a (0.18 to 0.25) and α_c(0.27 to 0.39), corresponding to the slope of the Tafel curves. The increase of α_a is due to the accelerated electron transfer process from bulk chalcopyrite to the surface layer, while the increase of α_c related to the upsurged diffusion rate of the oxidants toward the mineral surface.

Figure 6 shows the chalcopyrite electrochemical dissolution kinetics in Fe^{3+}-containing sulfuric acid solution. The former is larger when comparing the i_{corr} from Fe^{3+}-containing and Fe^{3+}-free acid solutions (Fig. 5). The i_{corr} increased from 67.60 to 97.72 μA cm^{-2} with 20% amplitude ultrasound introduced, which is about 45% of the increment. The equilibrium potential slightly shifted from 0.66 to 0.70 V. Comparing Fig. 6a and b, the part of the anodic reaction shows a vast difference in slope, with a much flatter slope for the curve of non-ultrasound. Statistically, the α_a was only 0.04 for the non-ultrasound curve and 0.21 for the ultrasound curve. The α_c slightly increased from 0.27 to 0.32 with ultrasound. The trend proved that the ultrasound had affected the anodic

reaction of chalcopyrite oxidation more than the cathodic reaction. The mechanism study of the phenomena will be conducted with different spectroscopy technologies in the next research.

Chalcopyrite Polarization in Sulfuric Acid Solution

CA was used to study ultrasound's effect on the chalcopyrite oxidation/Fe^{3+} reduction at controlled potentials. The time-dependent current density during the tests was registered, indicating the diffusion of the electroactive species towards the electrode surface.

The current density vs. time curves are plotted in Fig. 7 with 0.5, 0.6, 0.7, and 0.8 V applied potentials in sulfuric acid solution. The graph shows that all the curves drop sharply in the initial few minutes and slowly flattened as it approached 30 min. The rapid decrease is due to the electrochemically active species quickly diffusing to the working electrode's surface as a function of potential applied. The final current density at 30 min at all applied potentials was plotted as shown in Fig. 7c. At 0.5 and 0.6 V, where Fe^{3+} or dissolved O_2 reduction was the primary reaction, negative current densities were recorded. While at 0.7 and 0.8 V, anodic oxidation of chalcopyrite was the major reaction with positive current densities [40]. When the ultrasound was introduced, the final current densities increased from 4.36 to 9.51 μA cm^{-2} at 0.7 V and 9.24 to 23.8 μA cm^{-2} at 0.8 V. The results demonstrated that the ultrasonic wave could promote chalcopyrite electrochemical oxidation in the absence of Fe^{3+}. The promotion has been explained as the ultrasonic wave expedites the diffusion through the product layer [27]. More evidence is necessary for the mechanism exploration.

Chalcopyrite Polarization in Fe^{3+}-Containing Sulfuric Acid Solution

Similarly, CA tests were conducted at 0.5, 0.6, 0.7, and 0.8 V without and with ultrasound (20% amplitude) in 10 mM Fe^{3+}-containing sulfuric acid solution. The current density vs. time curves are shown in Fig. 8a and b. Figure 8c compares the final current density at 30 min with and without ultrasound. At 0.5 and 0.6 V, the reduction of Fe^{3+} to Fe^{2+} was the main reaction. At 0.5 V, the final current density was − 65.54 μA cm^{-2} without ultrasound, while it was − 1165.84 μA cm^{-2} with ultrasound. The 17.80 times increase in current density because ultrasound is attributed to the hastened Fe^{3+} diffusion process. The final current density difference with and without ultrasound substantially decreased at 0.7 V, close to the Fe^{3+}/Fe^{2+} redox potential of 0.77 V. At 0.7 V. The current densities overlapped by the anodic oxidation of chalcopyrite and cathodic Fe^{3+} reduction reaction. However, the ultrasound's acceleration of Fe^{3+} reduction reaction was still evident. At 0.8 V, the current represented mainly

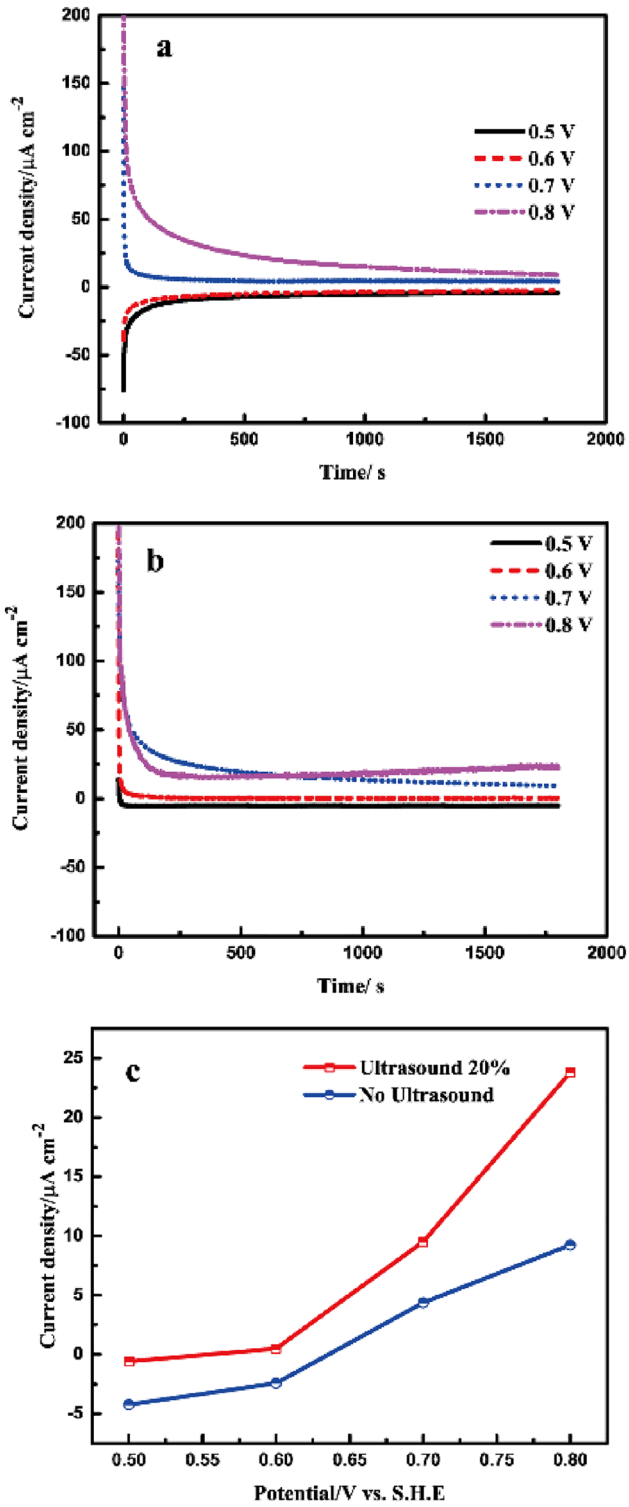

Fig. 7 Anodic polarization of chalcopyrite **a** without and **b** with ultrasound (20% amplitude) in 10 mM Fe^{3+} containing 0.5 M sulfuric acid solution. **c** Comparison of polarization current density at 30 min with and without ultrasound

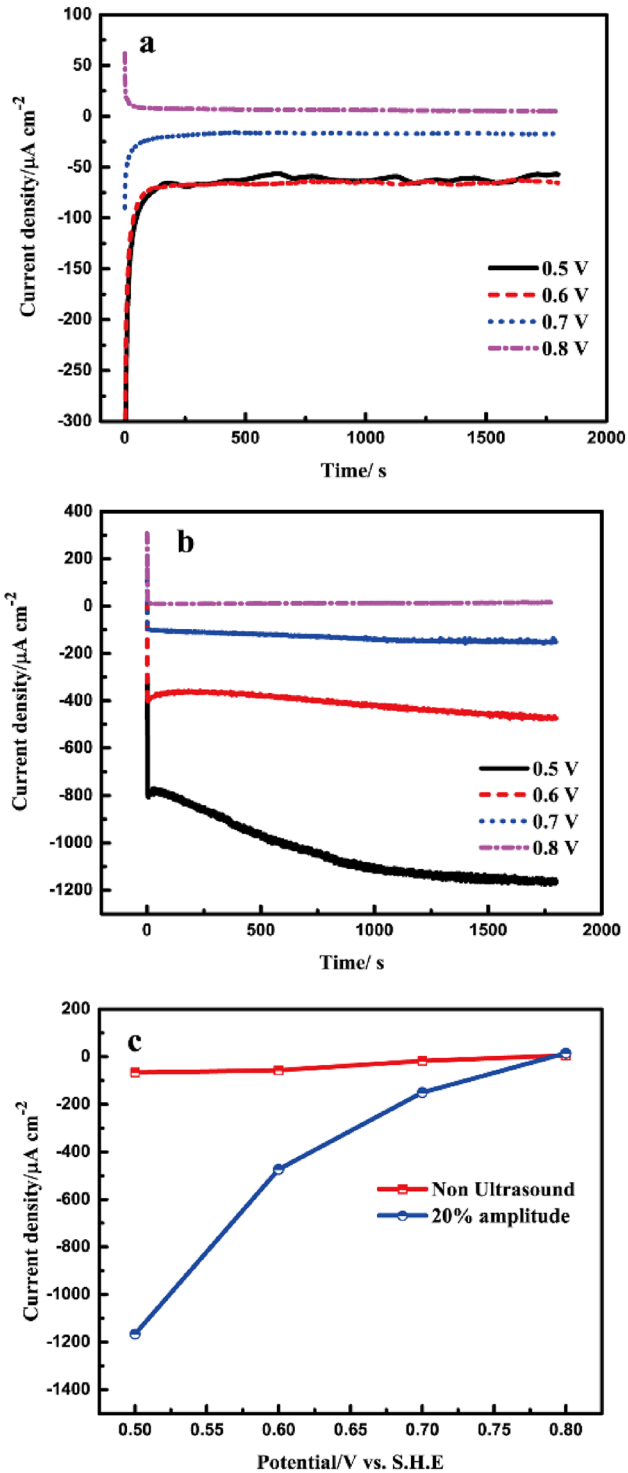

Fig. 8 Anodic polarization of chalcopyrite **a** without and **b** with ultrasound (20% amplitude) in 10 mM Fe^{3+} containing 0.5 M sulfuric acid solution. **c** Comparison of polarization current density at 30 min with and without ultrasound

the anodic reaction of chalcopyrite oxidation. It was still found that the ultrasound promotes chalcopyrite oxidation to some extent. At 0.8 V, the final current density without ultrasound was 5.22 μA cm^{-2}, while it was 15.49 μA cm^{-2} for the ultrasound test.

Conclusion

The conventional chalcopyrite oxidative leaching process suffers from slow kinetics, especially in sulfate media leaching systems. Ultrasound has been proven to be a feasible method to promote chalcopyrite leaching in acid solution. However, the kinetics study of ultrasound-assisted chalcopyrite leaching had not been studied from electrochemistry. This study compared the chalcopyrite ultrasound-assisted leaching kinetics with its electrochemical oxidation kinetics. The conventional UAL of chalcopyrite increased with the amplitude (20 to 60%) of ultrasound in both Fe^{3+}-containing and Fe^{3+}-free sulfuric acid solution. From the perspective of electrochemistry, linear sweep voltammetry with Tafel analysis and chronoamperometry tests were conducted for the electrochemical kinetics study. Tafel analysis shows the electrochemical dissolution rate of chalcopyrite increased about 45% with 20% amplitude ultrasonication power no matter if Fe^{3+} existed in the sulfuric acid solution. In addition, the CA tests found that ultrasound drastically increased the Fe^{3+} reduction reaction due to the accelerated Fe^{3+} diffusion onto the chalcopyrite electrode. This research provides an example for study of sulfide mineral oxidation kinetics with ultrasound assistance from the point view of electrochemistry.

Acknowledgements The authors wish to thank the National Research Council Canada's High-efficiency Mining program for financial support.

Funding Open Access provided by National Research Council Canada.

Declarations

Conflict of interest The authors declare no conflict of interest. The funders had no role in the design of the study, in the collection, analyses, or interpretation of data; in the writing of the manuscript; and in the decision to publish the results.

Open Access This article is licensed under a Creative Commons Attribution 4.0 International License, which permits use, sharing, adaptation, distribution and reproduction in any medium or format, as long as you give appropriate credit to the original author(s) and the source, provide a link to the Creative Commons licence, and indicate if changes were made. The images or other third party material in this article are included in the article's Creative Commons licence, unless indicated otherwise in a credit line to the material. If material is not included in the article's Creative Commons licence and your intended use is not permitted by statutory regulation or exceeds the permitted use, you will need to obtain permission directly from the copyright holder. To view a copy of this licence, visit http://creativecommons.org/licenses/by/4.0/.

References

1. Córdoba EM, Muñoz JA, Blázquez ML et al (2008) Leaching of chalcopyrite with ferric ion. Part I: general aspects. Hydrometallurgy 93:81–87. https://doi.org/10.1016/j.hydromet.2008.04.015
2. Li Y, Kawashima N, Li J et al (2013) A review of the structure, and fundamental mechanisms and kinetics of the leaching of chalcopyrite. Adv Colloid Interface Sci 197–198:1–32. https://doi.org/10.1016/j.cis.2013.03.004
3. Ji G, Liao Y, Wu Y et al (2022) A review on the research of hydrometallurgical leaching of low-grade complex chalcopyrite. J Sustain Metall 8:964–977. https://doi.org/10.1007/s40831-022-00561-5
4. Al-Harahsheh M, Kingman S, Al-Harahsheh A (2008) Ferric chloride leaching of chalcopyrite: synergetic effect of $CuCl_2$. Hydrometallurgy 91:89–97. https://doi.org/10.1016/j.hydromet.2007.11.011
5. Veloso TC, Peixoto JJM, Pereira MS, Leao VA (2016) Kinetics of chalcopyrite leaching in either ferric sulphate or cupric sulphate media in the presence of NaCl. Int J Miner Process 148:147–154. https://doi.org/10.1016/j.minpro.2016.01.014
6. Lu J, Dreisinger D (2013) Copper chloride leaching from chalcopyrite and bornite concentrates containing high levels of impurities and minor elements. Hydrometallurgy 138:40–47. https://doi.org/10.1016/j.hydromet.2013.06.001
7. Hua X, Zheng Y, Xu Q et al (2018) Leaching mechanism and electrochemical oxidation on the surface of chalcopyrite in ammonia-ammonium chloride solution. J Electrochem Soc 165:E466–E476. https://doi.org/10.1149/2.0711810jes
8. Torres D, Ayala L, Jeldres RI et al (2020) Leaching chalcopyrite with high MnO_2 and chloride concentrations. Metals (Basel) 10:107–119
9. Lundström M (2009) Chalcopyrite dissolution in cupric chloride solutions
10. Eghbalnia M (2012) Electrochemical and Raman investigation of pyrite and chalcopyrite oxidation, pp 1–201
11. Li J, Kawashima N, Kaplun K et al (2010) Chalcopyrite leaching: the rate controlling factors. Geochim Cosmochim Acta 74:2881–2893. https://doi.org/10.1016/j.gca.2010.02.029
12. Holmes PR, Crundwell FK (2013) Polysulfides do not cause passivation: results from the dissolution of pyrite and implications for other sulfide minerals. Hydrometallurgy 139:101–110. https://doi.org/10.1016/j.hydromet.2013.07.006
13. Lu D, Wang W, Chang Y et al (2016) Thermodynamic analysis of possible chalcopyrite dissolution mechanism in sulfuric acidic aqueous solution. Metals (Basel) 6:303. https://doi.org/10.3390/met6120303
14. Crundwell FK (2015) The semiconductor mechanism of dissolution and the pseudo-passivation of chalcopyrite. Can Metall Q 54:279–288. https://doi.org/10.1179/1879139515Y.0000000007
15. Hackl RP, Dreisinger DB, Peters E, King JA (1995) Passivation of chalcopyrite during oxidative leaching in sulfate media. Hydrometallurgy 39:25–48. https://doi.org/10.1016/0304-386X(95)00023-A
16. Li L, Liu G, Ghahreman A (2020) The interaction of Ag+ with synthetic chalcopyrite in the presence of Fe3+ and Cu2+ in sulfuric acid solutions. Electrochim Acta 338:135875. https://doi.org/10.1016/j.electacta.2020.135875
17. Turan MD, Sarı ZA, Nizamoğlu H (2021) Pressure leaching of chalcopyrite with oxalic acid and hydrogen peroxide. J Taiwan Inst Chem Eng 118:112–120. https://doi.org/10.1016/j.jtice.2020.10.021
18. Wang J, Faraji F, Ghahreman A (2021) Evaluation of ozone as an efficient and sustainable reagent for chalcopyrite leaching: process optimization and oxidative mechanism. J Ind Eng Chem 104:333–344
19. Ruiz-Sánchez A, Lázaro I, Lapidus GT (2020) Improvement effect of organic ligands on chalcopyrite leaching in the aqueous medium of sulfuric acid-hydrogen peroxide-ethylene glycol. Hydrometallurgy 193:105293. https://doi.org/10.1016/j.hydromet.2020.105293
20. Nazari G, Dixon DG, Dreisinger DB (2011) Enhancing the kinetics of chalcopyrite leaching in the Galvanox™ process. Hydrometallurgy 105:251–258
21. Yoo K, Kim S, Lee J et al (2010) Effect of chloride ions on leaching rate of chalcopyrite. Miner Eng 23:471–477
22. Luque-Garcıa JL, De Castro MDL (2003) Ultrasound: a powerful tool for leaching. TrAC Trends Anal Chem 22:41–47
23. Xiao J, Yuan J, Tian Z et al (2018) Comparison of ultrasound-assisted and traditional caustic leaching of spent cathode carbon (SCC) from aluminum electrolysis. Ultrason Sonochem 40:21–29
24. Swamy KM, Sarveswara Rao K, Narayana KL et al (1995) Application of ultrasound in leaching. Miner Process Extr Metallurgy Rev 14:179–192
25. Abed N (2002) The sonochemical leaching of chalcopyrite
26. Yoon H-S, Kim C-J, Chung KW et al (2017) Ultrasonic-assisted leaching kinetics in aqueous FeCl3-HCl solution for the recovery of copper by hydrometallurgy from poorly soluble chalcopyrite. Korean J Chem Eng 34:1748–1755
27. Ghahreman A, Wang J, Faraji F (2020) Effect of ultrasound on the oxidative copper leaching from chalcopyrite in acidic ferric sulfate media. Minerals 10:1–17. https://doi.org/10.3390/min10070633
28. Turan MD, Silva JP, Sarı ZA et al (2022) Dissolution of chalcopyrite in presence of chelating agent and hydrogen peroxide. Trans Indian Inst Met 75:273–280. https://doi.org/10.1007/s12666-021-02426-z
29. Ghahremaninezhad A, Asselin E, Dixon DG (2010) Electrochemical evaluation of the surface of chalcopyrite during dissolution in sulfuric acid solution. Electrochim Acta 55:5041–5056. https://doi.org/10.1016/j.electacta.2010.03.052
30. Li L, Bergeron I, Ghahreman A (2017) The effect of temperature on the kinetics of the ferric-ferrous redox couple on pyrite. Electrochim Acta 245:814–828. https://doi.org/10.1016/j.electacta.2017.05.198
31. Gu GH, Sun XJ, Hu KT et al (2012) Electrochemical oxidation behavior of pyrite bioleaching by Acidthiobacillus ferrooxidans. Trans Nonferrous Met Soc China (Engl Ed) 22:1250–1254. https://doi.org/10.1016/S1003-6326(11)61312-5
32. Lu J, Dreisinger D (2013) Copper leaching from chalcopyrite concentrate in Cu(II)/Fe(III) chloride system. Miner Eng 45:185–190. https://doi.org/10.1016/j.mineng.2013.03.007
33. Nakazawa H (2018) Effect of carbon black on chalcopyrite leaching in sulfuric acid media at 50 °C. Hydrometallurgy 177:100–108. https://doi.org/10.1016/j.hydromet.2018.03.001
34. Li L, Polanco C, Ghahreman A (2016) Fe(III)/Fe(II) reduction-oxidation mechanism and kinetics studies on pyrite surfaces. J Electroanal Chem 774:66–75. https://doi.org/10.1016/j.jelechem.2016.04.035
35. Stern HAG, Sadoway DR, Tester JW (2011) Copper sulfate reference electrode. J Electroanal Chem 659:143–150. https://doi.org/10.1016/j.jelechem.2011.05.014
36. Okur H, Tekin T, Ozer AK, Bayramoglu M (2002) Effect of ultrasound on the dissolution of colemanite in H_2SO_4. Hydrometallurgy 67:79–86. https://doi.org/10.1016/S0304-386X(02)00137-8
37. Bard AJ, Faulkner LR (1980) Electrochemical methods: fundamentals and applications. Wiley, New York
38. Tapera T, Nikoloski AN (2019) The effect of silver on the acidic ferric sulfate leaching of primary copper sulfides under recycle solution conditions observed in heap leaching. Part 4:

Semiconductor behaviour. Hydrometallurgy 186:50–57. https://doi.org/10.1016/j.hydromet.2019.03.016
39. Zhao H, Huang X, Wang J et al (2017) Comparison of bioleaching and dissolution process of p-type and n-type chalcopyrite. Miner Eng 109:153–161. https://doi.org/10.1016/j.mineng.2017.03.013
40. Yue G, Asselin E (2014) Kinetics of ferric ion reduction on chalcopyrite and its influence on leaching up to 150°C. Electrochim Acta 146:307–321. https://doi.org/10.1016/j.electacta.2014.08.060

Publisher's Note Springer Nature remains neutral with regard to jurisdictional claims in published maps and institutional affiliations.

Authors and Affiliations

Lin Li[1] · Aaron King[1] · Krystal Davis[1] · Ben Yu[1]

✉ Lin Li
lin.li2@nrc-cnrc.gc.ca

[1] National Research Council of Canada, Ottawa, ON K1A 0R6, Canada